ChemCatChem

Research Article
doi.org/10.1002/cctc.202200727

Chemistry Europe
European Chemical Societies Publishing

www.chemcatchem.org

Gold(I) NHC Catalysts Immobilized to Amphiphilic Block Copolymers: A Versatile Approach to Micellar Gold Catalysis in Water

Hanne Petersen,[a] Monika Ballmann,[b] Norbert Krause,*[b] and Ralf Weberskirch*[a]

Fifteen gold(I)-NHC-functionalized amphiphilic block copolymers that differ in the type of linker (ethyl, pentyl, octyl and benzyl) that attaches the gold(I) NHC catalyst to the block copolymer backbone, as well as, the substitution pattern of the NHC ligand (i.e. mesityl, methyl, 2,6-diisopropylphenyl and *n*-hexyl) were synthesized by a reversible addition and fragmentation transfer (RAFT) polymerization process. Micelle formation of the gold(I) NHC polymers was analyzed by electron microscopy and dynamic light scattering and revealed spherical and rod-like particles from 12 to 96 nm. In the micellar, gold(I) catalyzed cycloisomerization of an allene to the corresponding dihydrofuran, linker flexibility and substitution pattern of the NHC-ligand showed a strong effect on the catalytic activity. Best results were obtained were obtained for gold(I) NHC catalysts bound to the polymer backbone by pentyl linker whereas the rather stiff benzyl linker gave lowest catalyst conversion. Moreover, the polymer catalyst could be recycled in four consecutive runs and gave activities from 35 to 84% in the fourth run and underscores the importance of fine tuning structural parameters to achieve high conversion under micellar reaction conditions.

Introduction

In recent years, gold catalysis has become a versatile and efficient method in synthetic chemistry.[1] Typically, gold(I) and gold(III) salts as soft, carbophilic Lewis acids have been used that are capable of activating C–C double and triple bonds for inter- and intramolecular nucleophilic attack to enable efficient and selective access to new C–C or C-heteroatom bonds.[2] In recent years, many different approaches have been investigated to make gold catalysis more sustainable with the focus on recyclability as well as on the use of environmentally friendly reaction media. The recyclability of the catalyst can be achieved in many cases by binding the catalyst to support materials such as silica surfaces,[3] magnetic nanoparticles[4] or polymer networks.[5] Other approaches are based on the usage of ionic-liquids[6] or have been carried out under two-phase conditions,[7] whereby at the end of the reaction the catalyst and the product(s) are dissolved in different phases and can thus be separated from each other. In parallel, numerous attempts were made to perform gold catalysis in water as an environmentally friendly reaction medium. Therefore, gold(I) complexes with water-soluble ligands such as mono-, di-, and tri-sulfonated triphenylphosphine were tested.[8] Later, the focus shifted towards NHC-gold(I) catalysts that were modified with sulfonate groups,[9] cationic ammonium salts[10] and carbohydrate groups.[11] Micellar catalysis is another approach to combine recyclability of the catalyst with the usage of water as reaction medium.[12] Key to the success is the use of an appropriate amphiphile that can form micellar aggregates. Important examples are low molecular weight surfactants[13] such as CTAB or SDS, so called "designer" surfactants[14] that are PEGylated natural products, or amphiphilic block copolymers.[15] In particular, block copolymers have the advantage that they can be produced in a few steps with great variability in composition using living or controlled polymerization techniques.[16] Furthermore, the introduction of additional functional groups allows to covalently link the catalyst to the polymer backbone as a prerequisite for catalyst recycling.[16,17]

Few attempts have been made to transfer gold catalysis to a micellar environment. Lipshutz and Krause employed the designer surfactants PTS and TPGS-750 M and converted various α-functionalized allenes and alkyne diols to dihydrofurans and furans in a gold(III) catalyzed cyclization reaction.[18] Moreover, Krause and Weberskirch investigated the gold(III) catalyzed cycloisomerization of allenes in the presence of various amphiphilic poly(2-oxaoline)s and studied the effect of polymer composition and salt concentration on the overall product yield.[15a] However, the approach of just mixing a gold(III) salt with an amphiphile has some serious drawbacks: Firstly, the catalyst can leach during the reaction which makes catalyst recycling more difficult and secondly, the precise localisation (core, shell or interfaces) of the catalyst within the

[a] Dr. H. Petersen, Prof. Dr. R. Weberskirch
Faculty of Chemistry and Chemical Biology,
Polymer Hybrid Systems, TU Dortmund University
Otto-Hahn Straße 6, 44227 Dortmund (Germany)
E-mail: ralf.weberskirch@tu-dortmund.de
[b] Dr. M. Ballmann, Prof. Dr. N. Krause
Faculty of Chemistry and Chemical Biology,
Organic Chemistry, TU Dortmund University
Otto-Hahn Straße 6, 44227 Dortmund (Germany)
E-mail: norbert.krause@tu-dortmund.de

Supporting information for this article is available on the WWW under https://doi.org/10.1002/cctc.202200727

micelle remains unclear which makes it more difficult to better understand which structural parameters of the amphiphile or the catalyst ligand affect catalyst activity. While the first disadvantage can usually be compensated by adding fresh catalyst for each reaction cycle, the poor catalyst localisation can lead to lower catalyst activities.[19] An important alternative to the usage of gold salts are gold(I) NHC catalysts. Glorius et al. presented recently a surfactant-NHC-gold(I) system that has been successfully applied in the hydration of alkynes when further SDS was added to the reaction mixture and mixed head-to-head micelles were formed.[20] Due to the surfactant design the reaction most likely takes place at the micellar surface/water interface and is more suitable for hydrophilic substrates.

To broaden the applicability of micellar gold catalysis and better understand which parameters affect the activity of the gold catalysts we present here the synthesis and application of a new class of NHC(I) gold-functionalized, amphiphilic block copolymers. The synthesis scheme is particularly suitable for investigating the influence of certain parameters in particular the binding of the catalyst to the block copolymer and the ligand structure of the catalyst on the activity of these gold(I) NHC polymers under micellar reactions conditions. Therefore, fifteen gold(I)-NHC functionalized block copolymers were synthesized by a multistep RAFT-polymerization process and were investigated in the gold(I) NHC catalyzed cycloisomerization of various allenes to dihydrofuran derivatives.

Results and Discussion

Syntheses of the Gold(I) NHC catalyst active ester

Two strategies have been developed to covalently bind a catalyst to a polymeric support. These are based either on the synthesis of a monomer which already contains the ligand or the ligand-metal complex and can be polymerised directly into the block copolymer[19,21] or the ligand-metal complex is coupled to a functionalised block copolymer in a polymer analogue manner.[16a,17] Although the first approach is very elegant and allows excellent control over the amount of catalysts incorporated into the block copolymer, the synthetic effort for such monomers can be significantly higher[21] and some catalysts are not compatible with the respective polymerization mechanism. Therefore, we decided to immobilize our NHC-catalysts by a polymer analogue reaction to a functional block copolymer. One approach that has proven successful in the past is based on amine-functionalised block copolymers[22] and their polymer-analogue conversion with carboxylic acid functionalised ligands. To avoid the usage of coupling reagents we decided to use the gold(I)-NHC catalysts as active ester compounds. Therefore, in preliminary studies, we first compared the coupling efficiency of three active ester compounds, i.e. *p*-nitrophenyl, pentafluorophenyl and NHS ester. The three gold(I)-NHC active ester **1**–**3** were prepared according to literature procedures in a four-step synthesis (Scheme S1)[23] and were reacted with 1-aminohexane in a test reaction for 24 h at room temperature (Scheme 1). While both gold(I)-NHC complexes **2** and **3** showed good reactivities with quantitative conversion after 12 h, the reactivity of the *p*-nitrophenyl ester **1** was significantly lower which is in agreement with literature reports.[24]

Based on these results we chose to use the pentafluorophenyl ester (Pfp) system due to its higher overall yield in the three-step synthesis with 46% for compound **2** versus 24% for the NHS ester **3** and the possibility to detect any non-reacted compound **2** by ^{19}F-NMR spectroscopy. In the next step, four different gold(I)-NHC-catalysts **Cat1** to **Cat4** were prepared for the polymer-analogous immobilisation to a block copolymer precursor with sterically different substitution pattern on the NHC ring, i.e. mesityl (Mes), methyl (Me), 2,6-diisopropylphenyl (Dipp) and *n*-hexyl substituent, and were obtained in overall yields from 38% for the Dipp-substituted NHC ligand **Cat3** to 58% for the *n*-hexyl substituted NHC ligand **Cat4** (Scheme 2).

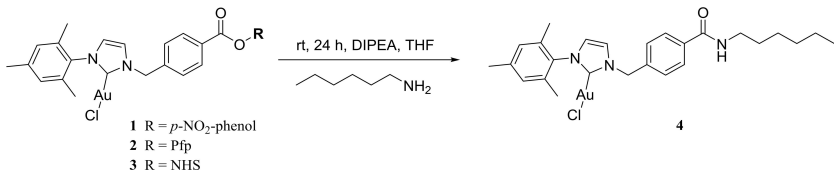

Scheme 1. Coupling reaction for three different gold(I)-NHC active ester **1**–**3** with 1-aminohexane.

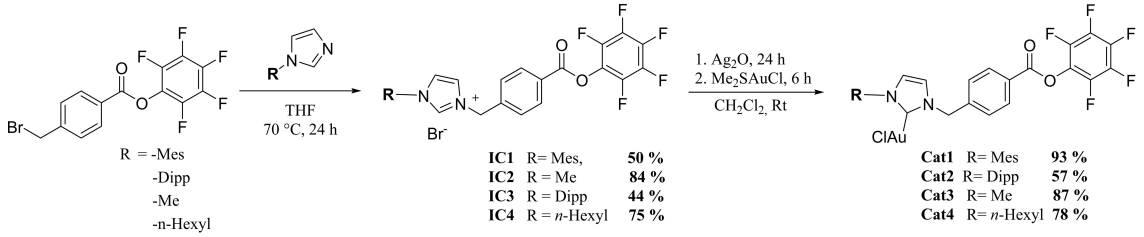

Scheme 2. Synthesis of NHC-gold(I) complexes **Cat1** to **Cat4**.

The chemical structures of the four gold catalysts were verified by ^{1}H-NMR, ^{13}C-NMR, and mass spectrometry.

A second important parameter that is known to affect catalyst activity is the linker between the metal-ligand complex and the block copolymer backbone.[22] Therefore, four Boc-protected amine functionalized monomers **M1** to **M4** were synthesized that differ in the length of their alkyl spacer ranging from two, five to eight methylene units (**M1** to **M3**) or in the rigidity by utilizing a benzyl linker (**M4**). All monomers **M1** to **M4** were prepared in a two-step synthesis and were characterized by ^{1}H-NMR and mass spectrometry (Scheme 3, Scheme S2). The Boc-protective group was chosen because it allows a reliable and quantitative determination of the amine component in the copolymer via the characteristic *tert*-butyl signal and can also be removed easily in a polymer analogous reaction.

Synthesis of the block copolymers

All block copolymers were synthesized by using the RAFT-polymerisation process according to a literature procedure by Laschewsky et al.[25] AIBN acted as the radical initiator and 2-cyano isopropyl dodecyl trithiocarbonate was used as RAFT agent (Scheme 3). The hydrophilic block was composed of dimethyl methacrylate (DMA) whereas the hydrophobic block contained a mixture of *n*-butyl acrylate (BuAc) and a Boc-protected amine acrylate **M1** to **M4**. The block copolymer is built by starting with the hydrophilic part consisting of DMA.

Five polyDMA macroRAFT polymers **MR1** to **MR5** were prepared with a block length ranging from 65 to 88 repeating units. They were all characterized by ^{1}H-NMR and SEC showing low dispersities Đ in a range between 1.09 and 1.18 which is typical for a controlled polymerization process (Table S1). The second block was polymerized by adding a mixture of *n*-butyl acrylate and one of the four monomers **M1** to **M4** to a solution of the macroRAFT **MR1** to **MR5** in dioxane and AIBN and let the polymerisation continue for 24 h at 80 °C. The block copolymers were finally characterized by ^{1}H-NMR spectroscopy and SEC (Table S2). A typical ^{1}H-NMR spectrum is shown in Figure 1.

The successful incorporation of the Boc-protected amino-functionalized monomer **M2** was confirmed with the signal at 1.43 ppm. Moreover, the quantification of the block copolymer composition and the determination of the molar mass were carried out by ^{1}H-NMR end group analysis based on the characteristic peak for the methyl groups of the DMA units at 2.92 ppm which served as a reference for the integrals of the other peaks. Thus, in all ^{1}H-NMR spectra of the block copolymers the integrals are normalized to the signal a. In total, we prepared five block copolymers **BP1** to **BP5** with a comparable composition and hydrophilic to hydrophobic balance (HLB) but they differ mainly in the type of linker that has been used to bind the NHC-gold(I) catalyst to the block copolymer backbone. The composition and analytical data are summarized in Table S2. The dispersity of the resulting block copolymers **BP1** to **BP5** was between 1.21 and 1.35 which are typical values for a RAFT polymerization.[25] Aggregate sizes from 1 mM aqueous solutions as determined by dynamic light scattering (DLS) were around 18.5 to 20.5 nm for **BP1** to **BP4**, only **BP5** with the benzyl linker formed larger aggregates in water with a diameter of 32.0 nm.

For the subsequent immobilization of the gold(I) NHC complexes **Cat1** to **Cat4**, we decided to remove the trithiocarbonate endgroup because coordination of the gold atom to the trithiocarbonate group can lead to an impairment of catalytic activity and should therefore be avoided.[26] Removal of the trithiocarbonate endgroup was carried out based on a method published by Moad et al. using AIBN and LPO as radical initiators.[27] The successful reaction was followed by UV-Vis spectroscopy by comparing the absorbance at 309 nm before and after the reaction (Figure S1). After Boc-deprotection of the block copolymers **BP1** to **BP5** with trifluoroacetic acid (TFA) it

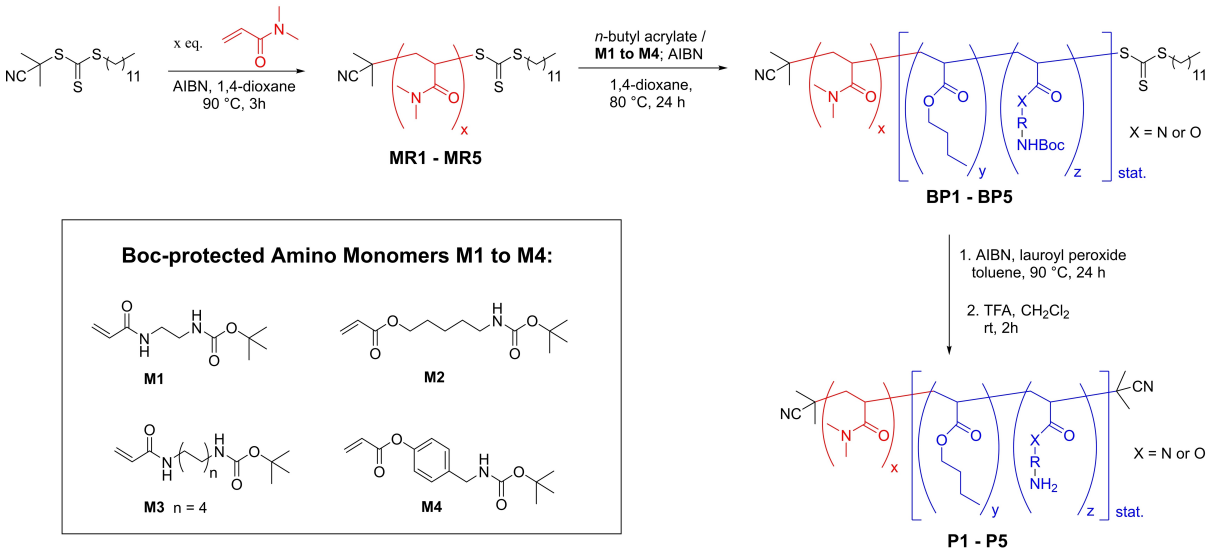

Scheme 3. Synthesis of amino-functionalized block copolymers **P1** to **P5** by a RAFT polymerization process.

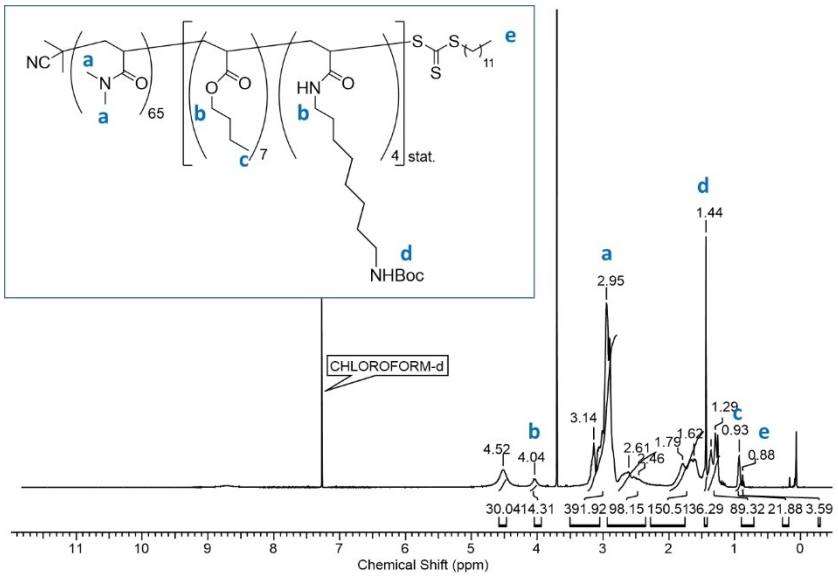

Figure 1. ^{1}H-NMR spectrum of **BP4** (in $CDCl_3$).

was important to neutralize the resulting polymer solution to pH ~ 7 with potassium carbonate because the gold(I) NHC complexes are very acid-labile and would otherwise decompose during immobilization. The deprotected block copolymers **P1** to **P5** were analyzed by ^{1}H-NMR spectroscopy and the absence of the broadened singlet at 1.43 ppm confirmed the successful removal of the BOC protection group. Furthermore, the BOC deprotection led also to a significant reduction in micelle size for the resulting amino-functionalized block copolymers **P1** to **P5** (Table S3). In the last step, the NHC-gold(I) catalysts **Cat1** to **Cat4** were coupled to the amino functionalized block copolymers **P1** to **P5**. The NHC-gold(I) complex was used in a slight excess (1.1 eq. relative to the amine functions in the copolymer) to ensure complete conversion of the primary amines and to avoid any coordination of gold atoms at the amino groups which would significantly reduce the catalytic activity (Scheme 4).

^{1}H-NMR spectroscopy confirmed the successful catalyst immobilization reaction as can be seen for catalyst **PC5** (Figure 2). Moreover, DOSY-NMR measurements in $CDCl_3$, gave a diffusion coefficient of 9.9×10^{-10} m^2s^{-1} confirming that there was only one polymeric species in solution and no low

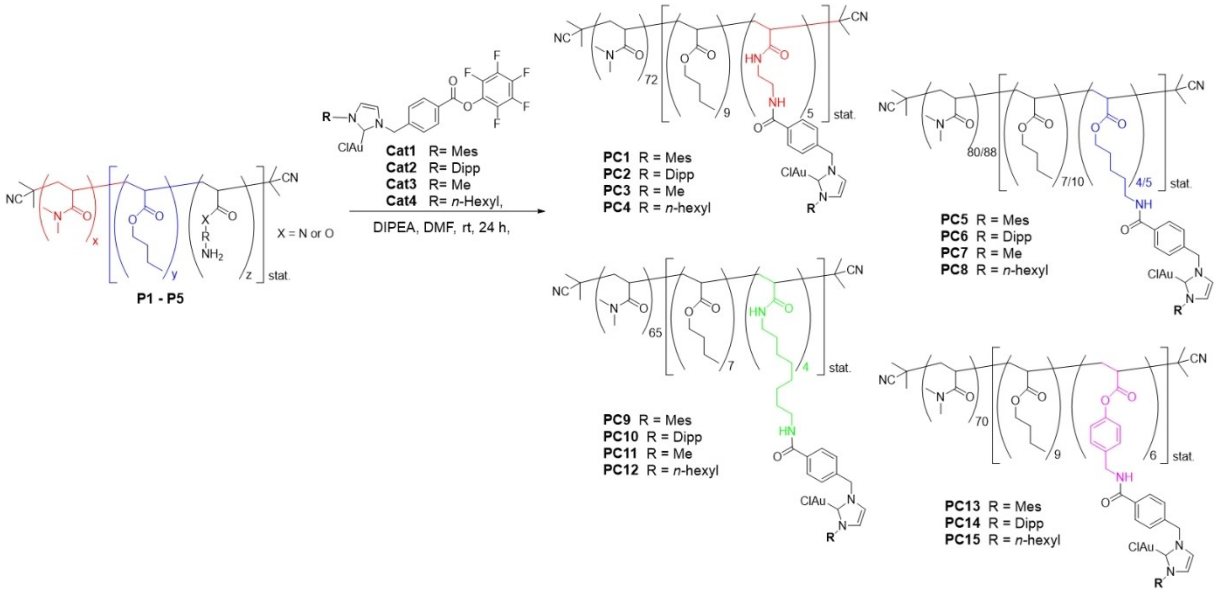

Scheme 4. Synthesis of the gold(I)-NHC functionalized block copolymers **PC1** to **PC15** based on precursor copolymers **P1** to **P5** and the catalysts **Cat1** to **Cat4**.

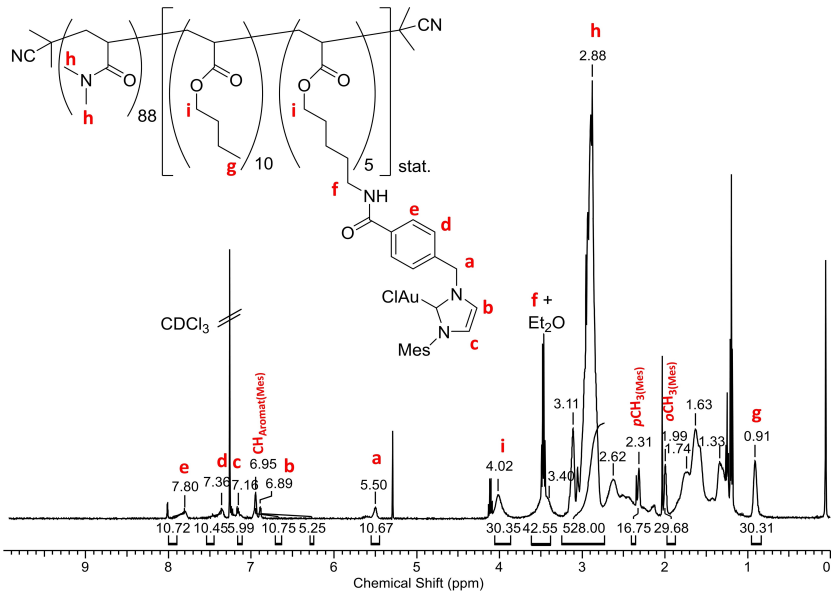

Figure 2. ^{1}H-NMR spectrum of **PC5** (in $CDCl_3$).

molecular weight catalyst anymore after purification of **PC5** by precipitation (Figure S2, Table 1).

We then investigated the aggregation behavior of **PC1** to **PC15** in aqueous solution using dynamic light scattering (DLS) and transmission electron microscopy (TEM) studies. The results clearly showed that both the catalyst and the linker influence the size and shape of the micellar aggregates. The DLS measurements reveal that the polymeric catalyst with the sterically less hindered gold(I) NHC catalysts with the methyl residue at the NHC-ligand form the smallest micellar aggregates in water with 11.9 to 29.3 nm in diameter, nearly independent of the linker length and flexibility (**PC3**, **PC7** and **PC11**). In contrast, the sterically demanding NHC ligands with dipp substituents (**PC2**, **PC6**, **PC10** and **PC14**) led to the largest micellar aggregates with hydrodynamic diameter of 50.9 nm (**PC10**) up to 96.4 nm (**PC14**), whereas the n-hexyl and mesityl series were somewhere in between. Next, we investigated the effect of different substituted gold(I) NHC catalyst (**PC1** to **PC4)** and the effect of linker length and flexibility (**PC1**, **PC5**, **PC9** and **PC 13**) on the shape of the micellar aggregates by transmission electron microscopy. As can be seen from Figure 3, only **PC1** with the sterically demanding mesityl group displayed worm-like aggregates in a micellar solution whereas all other catalyst showed the typical spherical aggregates. Interestingly, all polymeric catalysts that have been prepared with the mesityl functionalized NHC gold(I) ligand showed worm-like aggregates

Table 1. Analytical data of the polymeric gold(I) NHC catalysts **PC1** to **PC15**.

Poly@Cat	Polymer	Linker	Cat	M_n[a] [g mol^{-1}]	x, y, z[b]	d[c] [nm]	Yield [%]
PC1	P3	C2	Cat1	11,670	72, 9, 5	42.4 ± 11.2	86
PC2	P3	C2	Cat2	11,877	72, 9, 5	89.9 ± 4.4	92
PC3	P3	C2	Cat3	11,146	72, 9, 5	17.0 ± 2.5	58
PC4	P3	C2	Cat4	11,497	72, 9, 5	69.0 ± 5.4	86
PC5	P2	C5	Cat1	13,100	88, 10, 5	65.1 ± 10.3	n.d.
PC6	P1	C5	Cat2	11,770	80, 7, 4	77.2 ± 11.0	69
PC7	P2	C5	Cat3	12,580	88, 10, 5	29.7 ± 4.5	77
PC8	P1	C5	Cat4	11,909	80,7, 4	27.1 ± 13.3	61
PC9	P4	C8	Cat1	10,409	65, 7, 4	20.1 ± 2.3	74
PC10	P4	C8	Cat2	10,577	65, 7, 4	50.9 ± 11.9	57
PC11	P4	C8	Cat3	9,992	65, 7, 4	11.9 ± 2.8	51
PC12	P4	C8	Cat4	10,272	65, 7, 4	32.6 ± 7.2	55
PC13	P5	benzyl	Cat1	12,728	70, 9, 6	74.4 ± 12.8	68
PC14	P5	benzyl	Cat2	12,987	70, 9, 6	96.4 ± 13.0	50
PC15	P5	benzyl	Cat4	12,501	70, 9, 6	64.2 ± 8.0	68

[a] Determined by ^{1}H-NMR end group determination, [b] Copolymer composition as determined by ^{1}H-NMR: x = *N,N'*-dimethylacrylamide, y = *n*-butyl acrylate, z = catalyst containing monomer, [c] Determined by DLS measurements of a 1 mM polymer solution in MilliQ water.

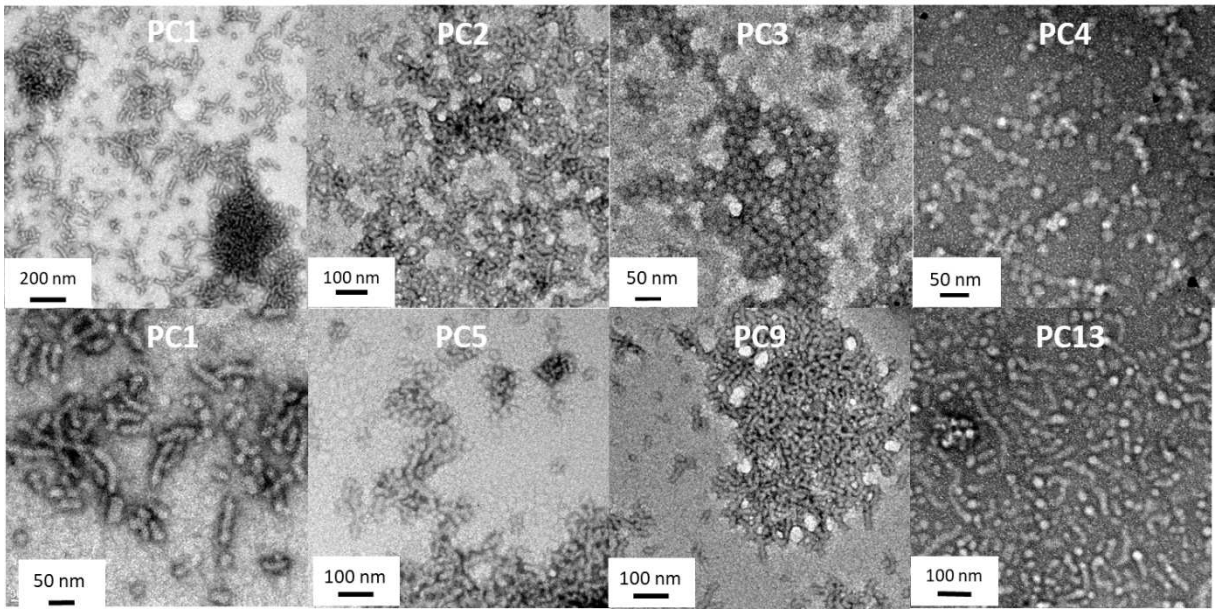

Figure 3. TEM images of the block copolymers micelles from polymer catalyst with different NHC substitution pattern, **PC1** (mesityl), **PC2** (dipp), **PC3** (methyl), **PC4** (*n*-hexyl) and different linker between gold(I) NHC catalyst and the block copolymer, **PC1** (ethyl), **PC5** (pentyl), **PC9** (octyl) and **PC13** (benzyl).

independent of the linker length (**PC1**, **PC5**, **PC9** and **PC13**, Figure 3). Similar effects of longer hydrophobic side chains on the shape of a micellar aggregate have also been reported in the literature, however, it is not clear so far if the transition from spherical to rod-like aggregates has any impact on the catalytic activity.[19]

Micellar catalysis

To explore the ability of the polymeric gold(I) NHC catalysts **PC1** to **PC15** to promote the gold-catalyzed cycloisomerization of functionalized allenes under micellar reaction conditions, the conversion of substrate **1a** into the corresponding dihydrofuran **2a** was chosen as benchmark reaction (Scheme 5).

First, we analyzed the impact of different reaction parameters on the catalyst activity under micellar conditions. Therefore, we started at a polymer concentration of 1 mM which is well above the critical micelle concentration (cmc) with 5 mol-% [Au] and analyzed the conversion of **1a** after 24 reaction time at room temperature in the presence of different silver additives. As can be seen from Table 2, the silver additives did not have any beneficial effect and substrate conversion was always reduced (Table 2, entry 2 to 4) compared to the reference (Table 2, entry 1). As expected, a very slow conversion was observed with silver hexafluoroantimonate alone (Table 2, entry 5). Next we examined the effect of polymer concentration on the reaction kinetics. Best results were obtained for a 1 mM polymer concentration of **PC4** whereas lower amphiphile concentration led to slower substrate conversion since the number of micellar aggregates as reaction centers should also decrease (Table 3). Finally, we analyzed effect of salt concentration which has been reported to influence the catalytic activity for many micellar catalyzed reactions.[28] As can be seen from Table 4, the addition of NaCl had no beneficial effect on substrate conversion and even reduced it from 93% (without NaCl, entry 2, Table 4) to 52%, 23% and 21% substrate conversion for 1, 3 and 5 mol-% NaCl addition, respectively

Table 2. Influence of polymeric NHC gold(I) catalyst **PC4** and different silver additives on the gold-catalyzed cycloisomerization of allene **1a** to the dihydrofuran **2a**.

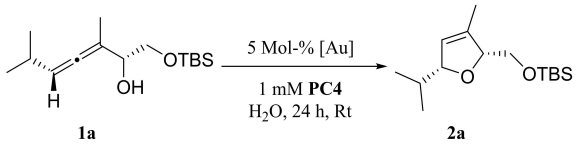

1a **2a**

Entry	[Au] [mol%]	Ag additive 5 mol%	Reaction time [h]	Conversion[a] [%]
1	5	–	24	quant.
2	5	$AgSbF_6$	24	71
3	5	AgOTf	24	80
4	5	$AgBF_4$	24	70
5	–	$AgSbF_6$	24	2

[a] As determined by ^{1}H-NMR spectroscopy.

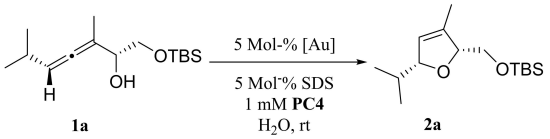

1a **2a**

Scheme 5. Cycloisomerization of allene **1a** into the corresponding dihydrofuran **2a** in the presence of the polymeric gold(I) NHC catalyst **PC4**.

Table 3. Influence of polymeric amphiphile concentration on the gold(I)-NHC catalyzed cycloisomerization of allene **1a**.

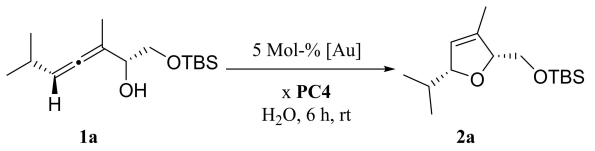

1a **2a**

Entry	Amphiphil [mM]	Conversion[a] [%]
1	2	88
2	1	93
3	0.5	50
4	0.125	12

[a] As determined by ^{1}H-NMR spectroscopy.

Table 4. Cycloisomerisation of α-hydroxyallene **1a** to 2,5-dihydrofuran **2a** using different NaCl concentrations.

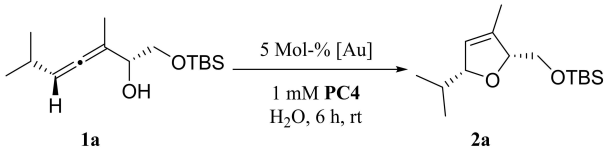

1a **2a**

Entry	T [°C]	c_{NaCl} [mol/L]	Conversion[a] [%]
1[b]	Rt	–	0
2	Rt	–	93
3	Rt	1	52
4	Rt	3	23
5	Rt	5	21
6	40 °C	–	96
7	40 °C	5	58

[a] Determined by means of ^{1}H-NMR spectroscopy; [b] Only with the block copolymer BP1.

(Table 4, entry 3–5). Also an increase in reaction temperature from room temperature to 40 °C could not fully compensate the negative effect of NaCl addition (Table 4, entry 7) and substrate conversion remained at 58 %. When using simple gold(III) salts such as $AuBr_3$, a significant increase in catalytic activity was observed which has been attributed to the possible stabilisation of ionic intermediates or transition states.[29] The opposite trend can be explained according to the results of Li et al. from 2015.[30] The equilibrium that forms between the neutral and cationic gold species is shifted to the side of the neutral species by the addition of sodium chloride, which leads to a reduction in the catalytic activity. Addition of organic co-solvents in order to increase the solubility of the starting material has no strong effect on the reaction rate (Table 5).

In the next set of experiments, we tested the effect of co-surfactants. Glorius et al. reported recently that the use of anionic co-surfactants such as sodium dodecyl sulphate (SDS) led to a considerable acceleration of the gold(I) NHC catalyzed micellar hydration of alkynes.[20] They postulated that the negative charge of the SDS head group stabilizes the cationic species of the NHC-Au(I) complex thus activating the catalyst. When we added between 10 to 50 μM sodium dodecyl sulfate (SDS, relative to the substrate) to the reaction mixture,

Table 5. Influence of organic solvents on the cycloisomerisation of allene **1a.**

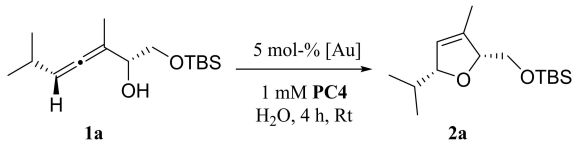

1a **2a**

Entry	Solvent	Conversion[a] [%]
1	–	75
2	10 % THF	77
3	10 % Toluene	45
4	10 % Acetone	51

[a] Determined by means of ^{1}H-NMR spectroscopy.

complete conversion of the allene was observed after 30 and 50 min (Table 6, entries 5–7). However, ^{1}H-NMR analysis showed the formation of an unidentified by-product in varying proportions. Therefore, we lowered the SDS concentration to 5 μM and extended the reaction time to 70 min and complete conversion could be achieved and no by-product formation was observed. When using the cationic surfactant cetyl trimethylammonium bromide (CTAB) the cycloisomerization was not accelerated and only 40 % conversion was achieved after 40 min reaction time comparable to the results without any co-surfactant. (Table 6, entry 11).

After optimizing the reaction parameters, we examined the effect of catalyst linkage to the polymer backbone and the effect of NHC substitution pattern on catalyst activity under micellar reaction conditions.

As can be seen from Table 7, best conversions were obtained after 40 min for those NHC ligands with *n*-hexyl substituent whereas the methyl, mesityl or dipp substituents

Table 6. Influence of different co-surfactants on the micellar cycloisomerization of allene **1a**.

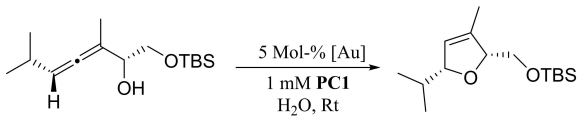

1a **2a**

Entry	Reaction time [min]	Co-Surfactant [mM]	Conversion[a] [%]
1	240	–	75
2	240	**P2**/0.5	15
3	240	**P2**/1.0	7
4[b]	1,440	**P2**/1.0	0
5[c]	30	**SDS**/40	>99
6[c]	40	**SDS**/20	>99
7[c]	50	**SDS**/8	>99
8	70	**SDS**/4	>99
9	40	–	42
10	40	**SDS**/4	78
11	40	**CTAB**/4	40
12[b]	1,440	**SDS**/40	3

[a] Determined by ^{1}H-NMR spectroscopy; [b] Control experiment without **PC1**, [c] Side product has been formed.

Table 7. Influence of imidazole substituents (Mes, Dipp, Me, *n*-hexyl) at constant alkyl and benzylic linker fragments on the cycloisomerization of α-hydroxyallene **1 a**.

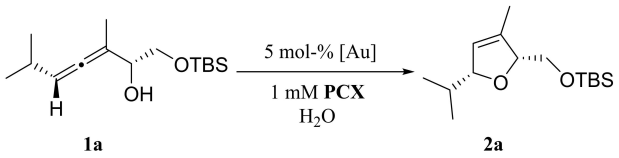

1a **2a**

				Conversion after 40 min[a] [%]		
Entry	Polymer	Linker	R	Rt	40 °C	Rt, 5 Mol-% SDS
1	**PC1**	-(C_2H_4)-	**Mes**	34	49	67
2	**PC2**	-(C_2H_4)-	**Dipp**	11	33	79
3	**PC3**	-(C_2H_4)-	**Me**	34	–	42
4	**PC4**	-(C_2H_4)-	***n*-hexyl**	46	56	62
5	**PC5**	-(C_5H_{10})-	**Mes**	40	56	78
6	**PC6**	-(C_5H_{10})-	**Dipp**	14	32	66
7	**PC7**	-(C_5H_{10})-	**Me**	26	17	77
8	**PC8**	-(C_5H_{10})-	***n*-hexyl**	48	70	72
9	**PC9**	-(C_8H_{16})-	**Mes**	5	31	54
10	**PC10**	-(C_8H_{16})-	**Dipp**	11	22	63
11	**PC11**	-(C_8H_{16})-	**Me**	26	52	47
12	**PC12**	-(C_8H_{16})-	***n*-hexyl**	44	47	74
13	**PC13**	-benzyl-	**Mes**	3	17	53
14	**PC14**	-benzyl-	**Dipp**	6	15	74
15	**PC15**	-benzyl-	***n*-hexyl**	17	34	64

[a] Determined by ^{1}H-NMR spectroscopy.

did not show clear trends. Notable, the presence of 5 mol% SDS as cosurfactant seems to dissolve the differences between the different catalysts and linkers and substrate conversions tend to equalize. Best results were obtained for **PC2 /SDS** with 79% conversion after 40 min whereas the worst system **PC3/SDS** showed 42% conversion (see Table 7, entry 2 and 3). Sterically more demanding substituents, like Dipp and Mes achieved lower conversion than alkyl groups like methyl or n-hexyl. The beneficial effect of SDS stems most likely from the fact that sodium dodecyl sulfate (SDS) is considered to be an acidic surfactant in the literature.[31] It has been reported that in neutral media, approximately 20% of the ion pair is dissociated in SDS-derived micelles, which leads to an increased proton concentration on the surface of the micelles[32] that has been found to be even higher when SDS was mixed with a neutral surfactants such as a neutral poly(ethylene oxide).[33] Since the addition of pTsOH has been reported to accelerate the gold-catalyzed dehydrative cyclization of acetylenic diols to furans,[34] the same effect of Brønsted acid-catalyzed reaction acceleration may also occur in the cycloisomerization of allenes in the presence of SDS. To better understand the effect of the linker between the catalyst and polymer backbone additional kinetic studies were performed on the cycloisomerisation of allene **1 a** to the furan **2 a**. As can be seen from Figure 4, there is a clear correlation between the type of linker and the resulting activities in a micellar gold catalysis in the following order: pentyl > ethyl > octyl > benzyl. This is in agreement with results published for other block copolymer catalyst systems that

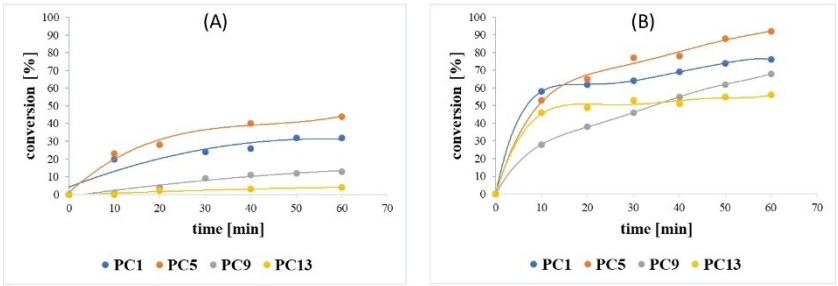

Figure 4. Kinetic study of the cycloisomerization of α-hydroxyallene **1 a** in the presence of block copolymers with different linkers between gold(I) NHC catalyst and polymer backbone: **PC1** = ethyl, **PC5** = pentyl; **PC9** = octyl and **PC13** = benzyl linker. (A) Reaction procedure at room temperature; (B) Reaction procedure at room temperature with 5 mol% SDS.

showed best activities with a C4 to C6 alkyl linker, whereas too short (ethyl) or too rigid linker (benzyl) led to significant decrease in catalyst activity.[19,21] T_1/T_2 relaxation studies support this assumption when the catalyst mobility of **PC5** (Cat 1 + pentyl linker) and **PC13** (Cat1 + benzyl linker) are compared showing the reduced mobility of the gold(I) NHC catalyst when bound to the polymer by a rather rigid benzyl linker (**PC13**) compared to the more flexible pentyl linker (**PC5**) (see also Figure S52).

Under these optimized conditions, various α-hydroxyallenes were converted into the corresponding furans in good yields of 62 to 89% within 40–150 minutes at room temperature in air (Figure 5).

Catalyst recycling

In the last part we examined the recyclability of the different polymer systems as a prerequisite of a sustainable process. Therefore, we carried out the cycloisomerization of the α-hydroxyallene **1 a** for 24 h followed by extraction with a mixture of pentane and diethyl ether to remove the product from the reaction solution. Any residual organic solvent was removed under reduced pressure after each recycle step before fresh allene substrate was added to the micellar solution and a new run was started. This procedure was repeated four times for each polymeric catalyst examined. First, we investigated the **SDS/ PC4** system which displayed one of the highest activities in the cycloisomerisation reaction. However, in the presence of SDS as an activating additive, a significant loss of catalyst activity was observed with each cycle and conversion for cycle 3 and 4 were 54% and 32%, respectively (Table S6). Moreover, we observed a rather strong foaming in the presence of SDS and subsequent phase separation took much longer time and was not always complete. Catalyst deactivation during the recycling procedure was further supported by a purple coloration of the reaction mixture which is probably caused by formation of gold nanoparticles. To increase the stability of the catalyst, SDS was not longer used and the reaction time was increased to 24 h to ensure quantitative conversion in the first run. As can be seen in Table S8, a significant improvement in reusability was observed. **PC1** achieved good to very good conversion over four reaction cycles (Table S8, entry 1; Figure 6 A). Only **PC9** and **PC13** showed a significant decrease in activity in the fourth run with 35% and 56%, respectively. In all cases, the catalytic activity decreased after the third run, but this could be compensated by extending the reaction times (Figure 6A, B). When investigating the effect of NHC substitution pattern on recyclability of the polymer catalyst, the overall trend of reduced catalyst activity in the third and fourth run could also be observed, however, the sterically more demanding mesityl (**PC5**) and dipp (**PC6**) substituents showed still more than 90% substrate conversion in the third run whereas the smaller methyl (**PC7**) and *n*-hexyl substituent (**PC8**) lost activity already in the third run most likely due the poorer shielding effect of gold center by the NHC ligand. Catalyst leaching, on the other hand, was recently investigated for **Cat1** covalently bound to the designer amphiphile PQS. In the gold-catalyzed cyclisation of alkynediols under micellar reaction conditions only minimal leaching from 0.3 to 8 ppm was found in 7 consecutive runs.[34]

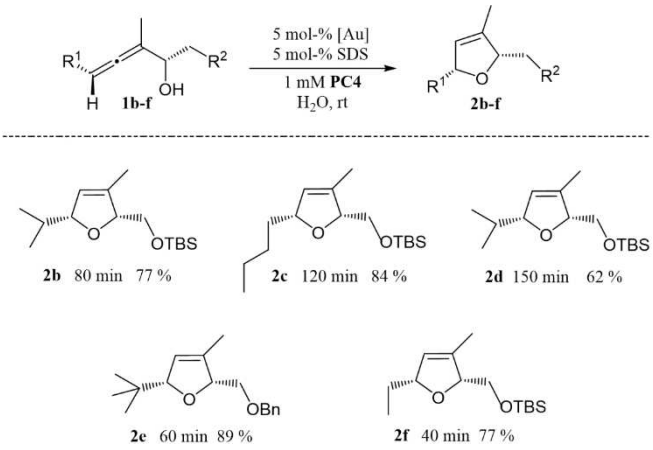

Figure 5. Time to full conversion and isolated yields of the gold(I) NHC-catalyzed cycloisomerization of various α-hydroxyallenes in the presence **PC4**.

Conclusions

In this work, gold(I) NHC functionalized block copolymers were synthesized and their application in the cycloisomerisation of α-allenols to their corresponding furans under micellar catalysis

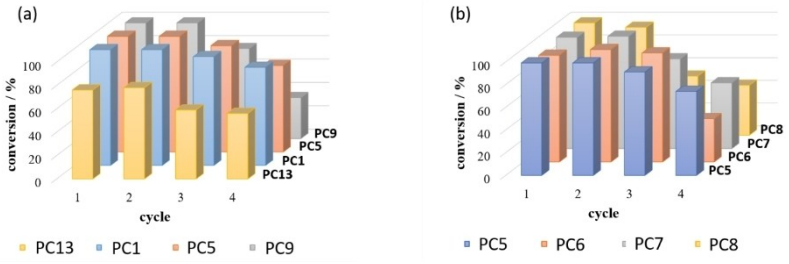

Figure 6. Recyclability of the different polymeric catalysts using the example of cycloisomerization of allene **1 a** in water. Reaction conditions: 5 mol% [Au], 1 mM polymer, 24 h each cycle, a) with varying linkers, **PC13** (benzyl), **PC1** (ethyl), **PC5** (pentyl), **PC9** (octyl) and b) substitution pattern of the NHC-ligand, **PC5** (mesityl), **PC6** (dipp), **PC7** (methyl) and **PC8** (*n*-hexyl).

conditions in water is described. Therefore, fifteen block copolymers with variable linker (ethyl, pentyl, ocytl and benzyl) between the catalyst and the polymer backbone, as well as, different steric properties at the *N*-heterocyclic carbene ligand (methyl, n-hexyl, dipp, mesityl substitution) were investigated. Amphiphilic block copolymer precursors were prepared by a controlled radical RAFT polymerization process. Coupling of the gold(I) NHC catalysts was achieved by reacting the gold(I) NHC active ester **cat1** to **cat4** with the amino group of the block copolymer precursor. The new block copolymer tagged NHC-gold(I) complexes showed excellent catalytic activity in cyclization reaction of functionalized allenes to the corresponding furans in bulk water. A pronounced acceleration of the reaction in the presence of the anionic co-surfactant SDS was observed. Moreover, clear correlations between catalyst activity and polymer structure was found, showing highest activities for polymeric catalysts with a pentyl linker and lowest activities for the benzyl linker whereas most active NHC ligands displayed *n*-hexyl substitution. Finally, recyclability of selected polymeric catalyst showed good to very good results in four consecutive runs.

Experimental Section

General working methods and chemicals

All chemicals were purchased from Sigma–Aldrich, TCI Europe, Alfa Aesar, Acros Organics, ABCR or Carl Roth and used without further purification unless noted in the text. Dry solvents such as THF, DCM, Et_2O, toluene and chloroform were purified and dried using the MB SPS 800 solvent drying system from M. Braun GmbH. The solvents were dried over activated aluminium oxide columns and removed under an inert gas atmosphere (argon). All other dry solvents were distilled over molecular sieves (3 Å) and stored under argon atmosphere. Technical solvents were previously distilled on a rotary evaporator. Moisture- and air-sensitive reactions were carried out in heated, septa-sealed Schlenk flasks or pressure Schlenk vessels under inert gas atmosphere (argon).

NMR spectroscopy

NMR spectroscopic investigations were carried out on Bruker FT-NMR instruments of the types AVANCE HD-III Nanobay (400 MHz), AVANCE HD-III (600 MHz) and with Agilent FT-NMR instruments of the type DD2 (500 MHz) at room temperature. The spectra were evaluated with the programme ACDLabs 12.0. The chemical shift δ is given in parts per million (ppm), the coupling constant J in Hertz (Hz). The calibration was performed on the residual protons of the deuterated solvent used, in this case deuterated chloroform (CDCl3: δ (1H) = 7.27, δ (13C) = 77.0) or deuterated benzene (C6D6: δ (1H) = 7.16). The following abbreviations were used to indicate the signal multiplicities: s = singlet, d = doublet, t = triplet, q = quartet, quin = quintet, dd = doublet of doublet, ddd = doublet of doublet of doublet, dt = doublet of triplet, m = multiplet, br. = broad.

Gel permeation chromatography

The GPC measurements were carried out using the L-5000 LC Controller, 655A-11 Liquid Chromatograph from Merck Hitachi. The eluent was DMF (HPLC grade + 5 g/L LiBr). It was measured over one precolumn (PSS GRAM) and two columns (PSS GRAM analytical 1000 Å and PSS GRAM analytical 30 Å) at a flow rate of 1 mL/min and a temperature of 60 °C. The eluent was calibrated with a PMC grade + LiBr. Calibration was performed using a PMMA calibration kit from Polymer Standards Service GmbH (PSS). Detection was carried out with the RI Detector Smartline 2300 from Knauer. Samples with a concentration of 3 mg/mL were prepared for the measurements. Before measurement, the samples were filtered with a 0.2 μm PTFE syringe filter.

High-resolution mass spectrometry

HR mass spectra were recorded on the THERMO LTQ Orbitrap from THERMO SCIENTIFIC with combined Accela HPLC system and enclosed Hypersil gold column (50 mm × 1 mm inner diameter, particle size 1.9 μm).

UV/Vis spectroscopy

UV/Vis spectroscopic measurements were performed on the UV-6300PC double beam spectrophotometer from VWR.

Transmission electron microscopy

TEM measurements were carried out by Mr. Volker Brandt in the working group of Prof. Dr. Tiller on the device CM200 of the company Philips equipped with the camera Orius SC200 of the company Gatan. 1 mM solutions of the respective polymers were measured. These were diluted in a ratio of 1 : 10 with distilled water. Water and then 20 μL of a sample was applied to a copper grid. The applied sample was carefully dried with a filter paper. Uranyl acetate was used as the contrasting agent.

Dynamic light scattering (DLS)

DLS measurements were performed on a NanoBrook ZetaPals Zeta Potential Analyzer from Brookhaven (He-Ne laser, $\lambda = 633$ nm, 25 °C). The measured polymer solutions were measured at a concentration of 1 mM, polymer nanoparticles at a concentration of 3 mg/mL. The BIC solutions software from Brookhaven was used to evaluate the measurement.

Fluorescence spectroscopy

Fluorescence spectrometric measurements were carried out with the fluorescence spectrometer Hitachi F-2700 in the working group of Prof. Tiller. The fluorescence probe used was 6-p-toluidino-2-naphthalenesulfonic acid (TNS). A stock solution of the polymer (1 mM) was prepared using a 2 μM TNS solution. A dilution series was then prepared starting from the stock solution, halving the concentration with each step. An increase in emission intensity at 415 nm indicated the formation of micellar structures in the solution. The spectra were evaluated with the software FL Solutions 4.1.

Supporting Information

Synthesis protocols for the monomers **M1**–**M4**, the catalysts **Cat1**–**Cat4** and the polymers are provided. Moreover, additional TEM images and ^{1}H, ^{13}C and ^{19}F-NMR spectra for selected intermediates and end products.

Acknowledgements

Open Access funding enabled and organized by Projekt DEAL.

Conflict of Interest

The authors declare no conflict of interest.

Data Availability Statement

Research data are not shared.

Keywords: gold catalysis · micelles · polymers · supported catalysts · sustainable chemistry

[1] a) A. S. K. Hashmi, G. J. Hutchings, *Angew. Chem. Int. Ed.* **2006**, *45*, 7896–7936; *Angew. Chem.* **2006**, *118*, 8064–8105; b) Z. C. Zu, T. T. Li, S. R. Mudshinge, B. Xu, G. B. Hammond, *Chem. Rev.* **2021**, *121*, 8452–8477; c) N. P. Nolan, *Acc. Chem. Res.* **2011**, *44*, 91–100.
[2] N. Krause, C. Winter, *Chem. Rev.* **2011**, *111*,1994–2009.
[3] a) E. de Canck, F. Nahra, K. Bevernaege, S. Vanden Broeck, J. Ouwehand, D. Maes, S. P. Nolan, P. van der Voort, *ChemPhysChem* **2018**, *19*, 430–436; b) J. T. Sarmiento, S. Suárez-Pantiga, A. Olmos, T. Varea, G. Asensio, *ACS Catal.* **2017**, *7*, 7146–7155.
[4] W. Yang, L. Wei, F. Yi, M. Cai, *Catal. Sci. Technol.* **2016**, *6*, 4554–4558.
[5] W. Wang, A. Zheng, P. Zhao, C. Xia, F. Li, *ACS Catal.* **2014**, *4*, 321–327.
[6] Ö. Aksın, N. Krause, *Adv. Synth. Catal.* **2008**, *350*, 1106–1112.
[7] W. Keim, *Green Chem.* **2003**, *5*, 105–111.
[8] S. Sanz, L. A. Jones, F. Mohr, M. Laguna, *Organometallics* **2007**, *26*, 952–957.
[9] E. A. Baquero, G. F. Silbestri, P. Gómez-Sal, J. C. Flores, E. de Jesús, *Organometallics* **2013**, *32*, 2814–2826.
[10] a) K. Belger, N. Krause, *Org. Biomol. Chem.* **2015**, *13*, 8556; b) K. Belger, N. Krause, *Eur. J. Org. Chem.* **2015**, *2015*, 220–225.
[11] H. Sak, M. Mawick, N. Krause, *ChemCatChem* **2019**, *11*, 5821–5829.
[12] a) G. La Sorella, G. Strukul, A. Scarso, *Green Chem.* **2015**, *17*, 644–683; b) T. Dwars, E. Paetzold, G. Oehme, *Angew. Chem. Int. Ed.* **2005**, *44*, 7174–7199; *Angew. Chem.* **2005**, *117*, 7338–7364.
[13] a) M. Vashishtha, M. Mishra, D. O. Shah, *Green Chem.* **2016**, *18*, 1339–1354; b) M. Banerjee, P. C. Panjikar, Z. T. Bhutia, A. A. Bhosle, A. Chatterjee, *Tetrahedron* **2021**, *88*, 132142.
[14] a) B. H. Lipshutz, S. Ghorai, M. Cortes-Clerget, *Chem. Eur. J.* **2018**, *24*, 6672–6695; b) N. R. Lee, M. Cortes-Clerget, A. B. Wood, D. J. Lippincott, H. B. Pang, F. A. Moghadam, F. Gallou, B. H. Lipshutz, *ChemSusChem* **2019**, *12*, 3159–3165.
[15] a) L. Lempke, A. Ernst, F. Kahl, R. Weberskirch, N. Krause, *Adv. Synth. Catal.* **2016**, *358*, 1491–1499; b) A. H. Lu, P. Cotanda, J. P. Patterson, D. A. Longbottom, R. K. O'Reilly, *Chem. Commun.* **2012**, *48*, 9699–9701; c) Y. Liu, V. Pinon III, M. Weck, *Polym. Chem.* **2011**, *2*, 1964–1975.
[16] a) B. M. Rossbach, K. Leopold, R. Weberskirch, *Angew. Chem. Int. Ed.* **2006**, *45*, 1309–1312; *Angew. Chem.* **2006**, *118*, 1331–1335; b) M. Klika Škopić, K. Götte, C. Gramse, M. Dieter, S. Pospich, S. Raunser, R. Weberskirch, A. Brunschweiger, *J. Am. Chem. Soc.* **2019**, *141*, 10546–10555.
[17] a) H. Sand, R. Weberskirch, *RCS Adv.* **2015**, *5*, 38235–38242; b) D. Schönfelder, O. Nuyken, R. Weberskirch, *J. Organomet. Chem.* **2005**, *690*, 4648–4655.
[18] a) S. R. K. Minkler, N. A. Isley, D. J. Lippincott, N. Krause, B. H. Lipshutz, *Org. Lett.* **2014**, *16*, 724–726; b) S. R. K. Minkler, B. H. Lipshutz, N. Krause, *Angew. Chem. Int. Ed.* **2011**, *50*, 7820–7823; *Angew. Chem.* **2011**, *123*, 7966–7969.
[19] M. Klika Škopić, C. Gramse, R. Oliva, S. Pospich, L. Neukirch, M. Manisegaran, S. Raunser, R. Winter, R. Weberskirch, A. Brunschweiger, *Chem. Eur. J.* **2021**, *27*, 1–11.
[20] A. Rihling, H.-J. Galla, F. Glorius, *Chem. Eur. J.* **2015**, *21*, 12291–12294.
[21] D. Schönfelder, K. Fischer, M. Schmidt, O. Nuyken, R. Weberskirch, *Macromolecules* **2005**, *38*, 254–262.
[22] M. Bortenschlager, N. Schöllhorn, A. Wittmann, R. Weberskirch, *Chem. Eur. J.* **2007**, *13*, 520–528.
[23] a) W. Niu, X. Chen, W. Tan, A. S. Veige, *Angew. Chem. Int. Ed.* **2016**, *55*, 8889–8893; *Angew. Chem.* **2016**, *128*, 9035–9039; b) J. Lemke, N. Metzler-Nolte, *Eur. J. Inorg. Chem.* **2008**, *21*, 3359–3366; c) J. Liu, J. Chen, J. Zhao, Y. Zhao, L. Li, H. Zhang, *Synthesis* **2003**, *17*, 2661–2666.
[24] J. Wang, R.-Y. Zhang, Y.-C. Wang, X.-Z. Chen, X.-G. Yin, J.-J. Du, Z. Lei, L.-M. Xin, X.-F. Gao, Z. Liu, J. Guo, *Synlett* **2017**, *28*, 1934–1938.
[25] C. Herfurth, P. Malo de Molina, C. Wieland, S. Rogers, M. Gradzielski, A. Laschewsky, *Polym. Chem.* **2012**, *3*, 1606–1617.
[26] a) A.-S. Duwez, P. Guillet, C. Colard, J.-F. Gohy, C.-A. Fustin, *Macromolecules* **2006**, *39*, 2729–2731; b) Z.-L. Wang, J.-T. Xu, B.-Y. Du, Z.-Q. Fan, *J. Colloid Interface Sci.* **2012**, *384*, 29; c) B. Ebeling, P. Vana, *Macromolecules* **2013**, *46*, 4862–4871.
[27] a) A. Postma, T. P. Davis, G. Moad, M. S. O'Shea, *Macromolecules* **2005**, *38*, 5371–5374; b) M. Chen, G. Moad, E. Rizzardo, *J. Polym. Sci. Part A* **2009**, *47*, 6704–7614.
[28] a) B. H. Lipshutz, S. Ghorai, *Aldrichimica Acta* **2008**, *41*, 59–72; b) B. H. Lipshutz, S. Ghorai, A. R. Abela, R. Moser, T. Nishikata, C. Duplais, A. Krasovskiy, R. D. Gaston, R. C. Gadwood, *J. Org. Chem.* **2011**, *76*, 4379–4391; c) B. H. Lipshutz, S. Ghorai, W. W. Y. Leong, B. R. Taft, D. V. Krogstad, *J. Org. Chem.* **2011**, *76*, 5061–5073.
[29] S. Handa, D. J. Lippincott, D. H. Aue, B. H. Lipshutz, *Angew. Chem. Int. Ed.* **2014**, *53*, 10658–10662; *Angew. Chem.* **2014**, *126*, 10834–10838.
[30] F. Li, N. Wang, L. Lu, G. Zhu, *J. Org. Chem.* **2015**, *80*, 3538.
[31] X. Hu, X.-S. Shu, X.-W. Li, S.-G. Liu, Y.-Y. Zhang, G. L. Zou, *Enzyme Microb. Technol.* **2006**, *38*, 675–682.
[32] B.-J. Kim, S.-G. Oh, M.-G. Han, S.-S. Im, *Langmuir* **2000**, *16*, 5841–5845.
[33] E. Iglesias, L. Montenegro, *Phys. Chem. Chem. Phys.* **1999**, *1*, 4865–4874.
[34] M. Ballmann, P. C. Ruer, O. Hofnagel, W. Hiller, N. Krause, *ACS Sustainable Chem. Eng.* **2022**, *10*, 7288–7298.

Manuscript received: June 7, 2022
Revised manuscript received: June 15, 2022
Accepted manuscript online: June 23, 2022
Version of record online: July 13, 2022